

# POSSIBILITIES OF USING THE POTENTIAL OF THE OCEANIC THERMAL ENERGY IN THE WATERS NEAR THE BORDERS OF MOZAMBIQUE

## POSIBILIDADES DE USO DEL POTENCIAL DE LA ENERGIA TÉRMICA OCEÁNICA EN AGUAS ALEDAÑAS A MOZAMBIQUE

A. W. FABIÃO<sup>a†</sup>, I. MITRANI<sup>b</sup>, J. CABRALES<sup>b</sup>

a) Instituto Superior Politécnico de Songo, Mozambique; americo.wilson@live.com.pt<sup>†</sup>

b) Instituto de Meteorología, 11700 La Habana, Cuba.

† corresponding author

Recibido 10/08/2017; Aceptado 22/11/2017

The present study explores the possibility of applying technologies of electricity generation from the ocean, using the thermal gradient energy in the Mozambique Channel (MC). For the application of this system, it is necessary a temperature difference around 20°C, between the surface and a lower level, with depth not greater than 1000 m. For this reason, the space and temporal behavior of the sea surface temperature was monthly analyzed for the period 1981-2016, including daily data during the year 2016. The ocean temperature in a depth of 1000 m, was analyzed too, for the same periods. The annual course of the ocean surface temperature and its spatial distribution were established. Three areas with a greater potential source of electricity generations were identified, which are located in the provinces of Inhambane, Nampula and Cabo Delgado, where the annual sea surface temperature varies from 24 to 28°C.

El presente trabajo explora la posibilidad de aplicación de tecnologías de generación de energía eléctrica a partir de la energía del gradiente térmico oceánico en el Canal de Mozambique (CM). Para la aplicación de este sistema es necesaria una diferencia de temperatura en el orden de 20°C, entre la superficie y un nivel inferior, con profundidad no mayor de 1000 m. Por esta razón, fue analizado el comportamiento espacial y temporal de la temperatura superficial para el período 1981-2016, y también los valores diarios para 2016, así como de la profundidad de 1000 m. Fueran identificadas las condiciones favorables, a lo largo de CM, en las costas de las provincias de Inhambane, Nampula y Cabo Delgado, donde la temperatura oceánica superficial anual varía de 24 a 28°C

PACS: Ocean energy extraction (Extracción de energía oceánica), 92.05.Jn; marine thermal gradients (gradientes térmicos marinos), 88.60.nj; ocean thermal energy (energía térmica oceánica), 88.60.nr

### I. INTRODUCTION

At present, concerns about environmental problems have been strongly reflected in scientific and academic debates. In the world order, it is an important action the search for different sources of alternative of energies that serve the domestic demand of the countries, which are not polluting or exhaustible. In this case, it is possible to opt for the sea resource of the sea. The generation of the energy from that resource of the water has different methods of implementation, from which they stand out: hydropower and oceanic energy. Among the types of the oceanic energy there is the energy of tides, waves, currents, salt gradient and thermal gradient.

All forms of energy generation, named above, use the kinetic or chemical energy of the waters for the electric generation. The oceans are large accumulators of solar thermal energy, where the temperature difference between the surface and the depth of several hundred meters generates a thermal gradient that can be used in oceanic thermoelectric plants, operating with fluids with low boiling point.

The first three meters of the ocean water mass accumulate more solar thermal energy than the whole atmosphere [1].

From data of ship expedition, carried out in the tropics, it has been known that the ocean surface contribution to the atmosphere, by evaporation, during the summer can be between 100 and 200 watt/m<sup>2</sup> [2], which is a considerably high value in comparison with the mechanical energy of the oceans (seas, currents and waves), which is on the order of  $3 \cdot 10^{-3}$  mW/m<sup>2</sup>.

This energy source can be extracted through an Ocean Thermal Energy Conversion (OTEC) process. For the application of this system, a temperature difference in the order of 20°C, between the surface and a lower level, with a depth of not more than 1000 meters [3] is necessary. Taking into account that the temperature in the depths of about one kilometer remains at around 4°C, this means that OTEC is particularly suitable when the average surface temperatures are around 25°C, typical of tropical latitudes [4,5].

For the operation of an OTEC installation, three processes can be differentiated: open cycle, closed cycle and hybrid systems. In an open-cycle plant, the hot water surface evaporates quickly and moves a turbine. The cold water is used to condense the steam again. The condensed desalted water can be used for various purposes (e.g. drinking water, irrigation). The cold water that has been pumped from the

depths of the sea can power an air conditioning systems after being used in the condenser. In addition, the cold sea water can also be used in aquaculture as it is rich in nutrients.

The closed cycle is the most used, being able to generate up to 40 MW, although it requires more equipment [1]. Closed cycle OTEC plants use a working fluid with a low boiling point, which is heated with warm water from the sea surface. The steam drives a turbine and condenses it using the cold water from the sea. In general, refrigerants or ammonia may be used as a working fluid, but the mixtures of water-ammonia are also used.

Hybrid OTEC systems consist of a combination of the open and closed cycles described above.

Mozambique has an extensive coastline, about 2,770 km long, and it has a considerable population density that lives on the coastal zone, where the generation of these types of energy can be used to support small businesses, fisheries, lighting in hospitals, schools and crop irrigation, among other applications. These technologies could be used not only for the electricity generation, but also for the direct production of drinking water or to meet thermal needs, such as cooling actions. In the country, studies about the use of ocean energies are scarce. Therefore, assessing its potential is the key to progress in technological development for its use. The present work explores the possibility of applying the electricity generation technologies from the energy of the oceanic thermal gradient in the Mozambique Channel.

The present work was taken under the following objectives:  
 a) To analyze the availability of thermal energy of the ocean, in the Mozambique Channel.  
 b) To characterize the affection by severe events, that could damage the facilities.  
 c) To determine the possible performance of a thermal machine and its theoretical maximum.

## II. DATA AND METHODS

### II.1. Background

The Mozambique Channel (MC) is a portion of the Indian Ocean that separates Madagascar from the rest of the continental region of the eastern of Africa, located on the western border of the coast of the Republic of Mozambique, between latitudes  $10^{\circ} 27'S$  and  $26^{\circ} 52'S$ , and lengths  $30^{\circ} 12'E$  and  $42^{\circ} 51'E$ . The coastline has a length of almost 2770 km. The Channel occupies approximately 460 km wide at the narrowest point between Mozambique and Madagascar, (Fig. 1). According to [6], in the Mozambique Channel a humid and sub-humid tropical climate is manifested with two seasons: the austral winter (dry season) and the austral summer (rainy season).

### II.2. Marine current system in the Mozambique Channel

The main currents in the Mozambique Channel and the circulation pattern are shown in Fig. 2. The shore line sinuosity generates an anticyclonic circulation, where the

surface warms the water is trapped. The southward flow in the central part of the Mozambique Channel, known as the Mozambique stream, joins the eastern Madagascar zone, as a narrow but well-defined fringe, derived from the South Equatorial Stream (SEC) which is divided into the Northeast Coast of Madagascar as the North-Eastern Madagascar Current (NEMC), where approximately 40% of the water mass is moved to the south as the Southeast Madagascar Current (SEMC) and Agulhas Current (AC).



Figure 1. Study area and limits of Mozambique, being to the north: Tanzania; Northwest: Malawi and Zambia; West: Zimbabwe, Southern Africa and Swaziland and East: Indian Ocean (Mozambique Channel).

### II.3. Data

The Sea Surface Temperature (SST), daily measure from satellites during the period 1981-2016, at the National Ocean and Atmosphere Administration (NOAA) archive, is available online at the website (<https://www.ncdc.noaa.gov/oisst>). This data appear in Network Common Data Form (NetCDF) format, with a space resolution of 1 km.

With the objective of establishing the temporal variation of the temperature in the depth of 1 km, the data of the daily average temperature on this level was obtained from the World Ocean Atlas, version 2 (WOA13 V2), freely available on the website (<https://www.nodc.noaa.gov/OC5/woa13/>).

To appreciate more details on the annual cycle, a TSS data was selected as study case for the year 2016.

## II.4. Data processing and analysis

Data processing was done, using the Grid Analysis and Display System, (GrADS) version 2.0.1, developed by the Center for Studies of the Earth-Ocean-Atmosphere System at the University of Maryland in the United States. The following particularities were determined:

- Spatial distribution of SST, its monthly and annual average, during the period 1981- 2016 (35 years).
- The Mapping of sea water temperature at the surface and 1000 m levels, including their annual and monthly averages for the period 1981-2016 and study case 2016.
- The calculation of the distance from the coast line to the isobaths with a depth of 1000 m, in order to determine the most suitable locations for the OTEC installation.

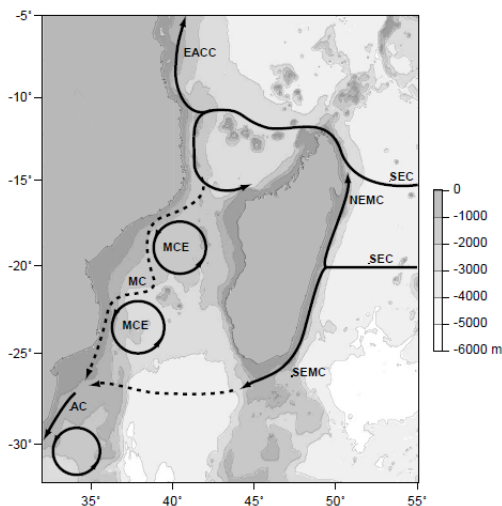


Figure 2. Model of circulation and main currents in the Mozambique Channel. South Equatorial Current (SEC), Southeast Madagascar Current (SEMC), Northeast Madagascar Current (NEMC), Mozambique Current (MC), the Agulhas Current (AC) and the Mozambique Channel eddies (MCE) [7].

The content energy was determined in a unit area column, applying the equation proposed by [8]

$$C_e = \rho_w C_p \Delta Z \Delta T, \quad (1)$$

where  $\rho_w$  is the mean sea water density ( $1030 \text{ kg m}^{-3}$ ),  $C_p$  is the specific heat at constant pressure of sea water ( $4 \times 10^3 \text{ J/kg } ^\circ\text{C}$ ), [9–11],  $\Delta Z$  is the thickness of the column of the water, which in this case is 1000 m and  $\Delta T$  is the temperature difference between the surface and 1000 m.

## II.5. Principle of operation of OTEC

The OTEC works with a liquid such as the ammonia, which has a boiling point smaller than that one of the water. The ocean surface is enough warm to heat the working fluid and cause a thermodynamic cycle of a thermal engine to produce electricity [12]. The condenser receives the deep ocean waters, from about 1000 meters deep, considering that

the temperature at this level is approximately  $4^\circ\text{C}$ . The cycle scheme is presented in Fig. 3. The efficiency of the installation will be evaluated by the thermodynamic principles presented by [13].

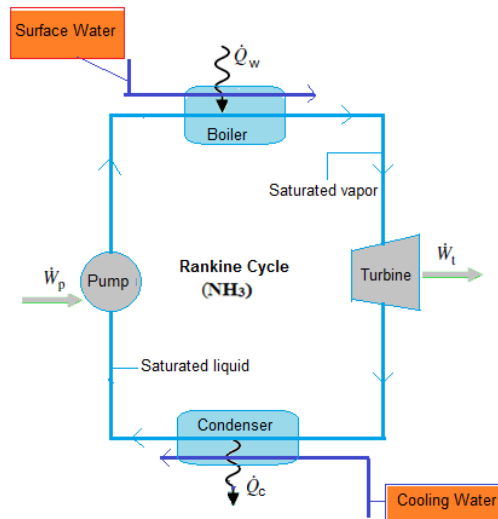


Figure 3. Schematic of the OTEC System.

## II.6. Performance of a thermal machine

The possible efficiency for the maximum, minimum and the annual mean TSS was determined. It was evaluated through the ideal Rankine cycle (Fig. 4). There are four main states in a Rankine cycle, and four main processes.

- 1-2 The isentropic compression in the pump to the state of the compressed liquid at the state of the compressed liquid at the pressure of the boiler.
- 2-3 The working liquid is boiled to change phase from a liquid to a saturated vapor.
- 3-4 The isentropic expansion of the working fluid through the turbine, from the superheated steam condition to the condenser of pressure.
- 4-1 The saturated liquid-vapor mixture is condensed back down to saturated liquid.

Table 1 shows the data used for the period between of 1981 and 2016, and the year 2016.

Some calculations of the specific enthalpy at various points, the power pump, fluid flowing pump, the cycle efficiency and the Carnot efficiency were performed based on the ideal Rankine cycle system. In this analysis, an OTEC plant with a capacity of less than 10 MW will be considered, the mass flow rate of the working fluid of 1000 kg/s will be taken into account. At the point 1 of the diagram, the ammonium temperature corresponds to the saturated liquid state, whereby the values of the specific enthalpy, the entropy

and the specific volume of ammonia are obtained in the tables of saturated ammonia.

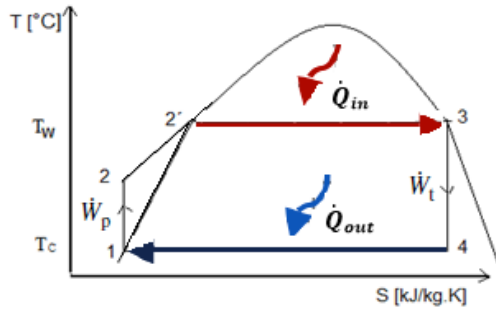


Figure 4. Diagram of Temperature vs Entropy (T-S), adapted from [13].

At the point 3, the increasing working fluid temperature was considered, due to the exchange of heat of the condensed

ammonia for the hot surface. It is considered an approximate value of steam saturated ammonia temperature and the values of specific enthalpy, entropy and pressures of points 1 and 3 are found in the tables of saturated ammonia vapor.

To solve the specific enthalpy at the point 4, we need to use the quality equation expressed as  $(X_4)$ . Quality refers to the mass fraction of steam to liquid in the saturated mixture. The Equation (2) uses the isentropic assumptions entropy, which is a known thermodynamic property at state 4, to calculate  $X_4$ . The specific enthalpy at the point 4 can be solved as it follows

$$S = S_f + X_4(S_{fg}), \quad (2)$$

$$h_4 = h_f + X_4(h_{fg}). \quad (3)$$

The subscript “f” indicates the liquid state and “fg” is a state of mixing liquid and vapor.

Table 1. The specific enthalpy in the different points of the T-S diagram, for different values of working fluid temperature, with TW water temperatures (annual maximum, average and minimum) and deep water temperature, TC.

North Region (Pemba, Nacala, Angoche) Period 1981-2016						
$T_w$ [°C]	$T_c$ [°C]	Diagram points	$h_1$ [kJ/kg]	$h_2$ [kJ/kg]	$h_3$ [kJ/kg]	$h_4$ [kJ/kg]
28.0	6.4	Specific Enthalpy values	293.28	298.25	1463.5	1382.15
28.8	6.4	Specific Enthalpy values	293.94	299.54	1461.21	1413.82
26.0	6.4	Specific Enthalpy values	226.75	227.18	1460.55	1411.59
Period 2016						
28.0	6.4	Specific Enthalpy values	293.28	298.25	1463.5	1382.15
30.0	6.4	Specific Enthalpy values	293.45	299.77	1463.5	1394.23
26.0	6.4	Specific Enthalpy values	226.75	227.18	1460.55	1411.59
South Region (Inhambane) Period 1981-2016						
28.0	4.8	Specific Enthalpy values	1463.9	1414.5	227.8	228.27
27.9	4.8	Specific Enthalpy values	293.45	298.25	1463.5	1382.15
24.0	4.8	Specific Enthalpy values	226.75	226.36	1459.9	1418.33
Period 2016						
26.5	4.8	Specific Enthalpy values	1463.9	1414.5	227.8	228.27
28.5	4.8	Specific Enthalpy values	226.75	227.29	1461.21	1413.68
24.0	4.8	Specific Enthalpy values	226.75	226.36	1459.9	1418.33

During the steady-state operation, the entire mass is preserved in both the water and the working sides. The mass flow rate ( $\dot{m}$ ) of the working fluid, flowing into the pumps, turbines and heat exchangers is equal to the flowing out, [14]. Therefore it is constant and assumed constant in all the stages of the power cycle. Now, the turbine power can be obtained through the following expression

$$\dot{W}_T = \dot{m}(h_3 - h_4) \quad (4)$$

For the compressed liquid point 2, the energy of the pump at the inlet and the power of the pump, with the specific enthalpy, will be calculated

$$W_P = -v(p_2 - p_1). \quad (5)$$

With the energy of the pump and the specific enthalpy at the input of the control volume, we calculate the specific enthalpy at the output of the control volume, by the following equation

$$h_2 = W_P + h_1. \quad (6)$$

Now, through the relation of the mass flow rate of the working fluid with the specific enthalpy change in points 1 and 2, we calculate the work entered by the pump

$$\dot{W}_P = \dot{m}(h_2 - h_1). \quad (7)$$

Now you proceed to determine the heat supplied ( $Q_{in}$ ) and the heat itself of the heat exchanger ( $Q_{out}$ ).

$$\dot{Q}_{in} = \dot{m}(h_3 - h_2), \quad (8)$$

$$\dot{Q}_{out} = \dot{m}(h_4 - h_1), \quad (9)$$

The thermal efficiency of a power plant is defined by the ratio between the useful power produced by the plant and the heat entering the plant. In the case of an OTEC plant, the thermal power supplied to the working fluid is from hot water, so that cycle efficiency of an OTEC plant can be given by

$$\eta_{ciclo} = \frac{\dot{W}_T - \dot{W}_P}{\dot{Q}_{in}}. \quad (10)$$

The efficiency of Carnot is a maximum theoretical efficiency. The Carnot cycle assumes that isentropic compression

is followed by a reversible heating, then the isentropic expansion, and finally a reversible cooling. A Carnot cycle is perfectly representative of a Rankine cycle since the working fluid must be preheated before it can be phase shifted but it provides the upper limit of the efficiency that can be obtained from the available thermal resource. The Efficiency of the Carnot is represented with the following equation

$$\eta_{Carnot} = \frac{T_W - T_C}{T_W}, \quad (11)$$

where  $\dot{m}$  is the mass flow rate of the working fluid (kg/s),  $v$  is the specific volume of ammonia ( $\text{m}^3/\text{kg}$ ),  $p_1, p_2$  are the pump inlet and outlet pressures (kPa),  $h_1, h_2, h_3$  and  $h_4$  are the specific enthalpy (kJ/kg),  $Q_{in}$  and  $Q_{out}$  are heats at the boiling and condensation (kW), and  $T_W$  and  $T_C$  are the absolute temperature from warm and cold water ( $^{\circ}\text{C}$ ).

### III. RESULTS AND DISCUSSION

#### III.1. Sea Surface Temperature

The maps SST in the waters of the Mozambique Channel (MC) show a latitudinal variation, so that for the northern region temperatures are higher than in the southern ones.

Fig. 5 A, B, C shows the annual average temperature distribution and the months of the maximum and minimum values. In Fig. 5A as an annual average, the SST can be seen with a range of  $24.5^{\circ}\text{C}$  in the southern zone, which increases to  $28^{\circ}\text{C}$  in the northeastern part of the MC, towards the coast of Madagascar. The figure Fig. 5C shows that during the winter, the SST over this area can be lower than  $23^{\circ}\text{C}$ , although in summer it rises to just over  $26^{\circ}\text{C}$ . This almost latitudinal distribution, responds to the regional oceanic circulation, typical of this tropical zone.

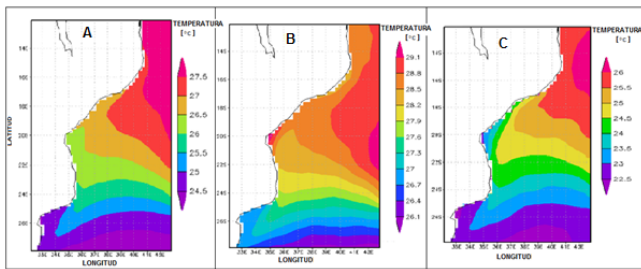


Figure 5. Marine Surface Temperature, averaged over the 1981- 2016 period for the MC, where **A** Annual average, **B** average maximum value, January month, **C** average minimum value, July month.

The coldest SSTs were recorded in the southern region (Maputo Bay and Inhambane, around the  $24^{\circ}\text{C}$ ) of the Channel, which during the year vary from  $23.5$  to over  $27^{\circ}\text{C}$ . The warmest ones, correspond to the centre and north, (Sofala Bank, Nacala and Pemba) from  $26^{\circ}\text{C}$  to over  $29^{\circ}\text{C}$ .

Fig. 6 shows the SST behavior of the southern, central and northern region of the Mozambique Channel, where the coldest SST are recorded for the southern region with respect to the central and northern regions.

In Fig. 6, the SST during the year 2016 presents a similar behavior as during the period 1981-2016. It is almost latitudinal, with values from  $24^{\circ}\text{C}$  in the southern region, to  $28.5^{\circ}\text{C}$  in the northeast of the MC.

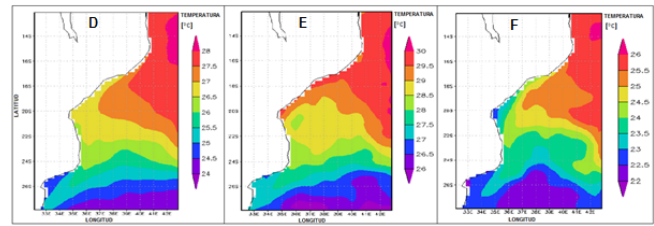


Figure 6. The Marine Surface Temperature, corresponding to the year 2016, averaged for the MC, where **D** The Annual average, **E** The Maximum value average, observed in January, **F** The Minimum value average, observed in July.

The SST varies from  $25^{\circ}\text{C}$  in the areas near the Mozambican coast to more than  $28^{\circ}\text{C}$  in the northeast of the MC, around Pemba, near the northwest coast of Madagascar, (Fig. 6D). The highest values were recorded in the northern region of MC, possibly due to the input influence of the South Equatorial Current (SEC), which is the main source of water mass supply from the upper layer of oceanic waters to the MC. In this year, the coldest SSTs were recorded in the southern region of Channel (Maputo Bay and Inhambane), with values ranging from  $25$  to  $26.5^{\circ}\text{C}$  during the year and the warmest in the central and northern areas (Sofala Bank, Angoche, Nacala and Pemba), from  $27$  to  $28^{\circ}\text{C}$ . Map on Fig. 6E shows hot surface waters during the summer, with SST ranging from  $26^{\circ}\text{C}$  to  $28^{\circ}\text{C}$  for the southern region near the Mozambican coast and from  $29^{\circ}\text{C}$  to  $31^{\circ}\text{C}$  in the central and northern region of the MC, along the coast of Madagascar. Map on Fig. 6F illustrates the variation of the temperature during the month of July, for the winter, with surface temperatures varying from  $22^{\circ}\text{C}$  to  $24^{\circ}\text{C}$  for the southern Channel region, and from  $24.4^{\circ}\text{C}$  to  $27^{\circ}\text{C}$  for central and the northern Channel region.

Along the MC, the relatively highest surface temperatures in the neighborhood of the Madagascar region, in the northwest of the MC, but also the strongest gradients towards the south of the Channel, are observed. This situation is attributed to the fact that warmer waters are transported by the northern branch of the Madagascar current and according to [6, 15], along the MC, the transport is characterized by two different water masses. From the north comes the Southern Equatorial Current that is incorporated into the Madagascar current, but in the south the waters penetrate coming from the center with subtropical anticyclonic turn at the Indian Ocean. In Fig. 2 are present the main current system that contribute to the variation of the water in the MC. The annual temperature oscillations are generated with a range of  $2-5^{\circ}\text{C}$ , in accordance with the description of [16].

#### III.2. Deep water temperature

The behavior of the temperature in the depth of 1000 m, along the MC, shows that this temperatures are colder in the south than in the north.

Fig. 7 illustrates the space temperature distribution in the depth of 1 km (cold waters), for the entire MC. It is observed that the temperature varies from 4.6 to 6.8°C. These temperatures are typical for tropical and subtropical regions in these depths. As a positive balance, it should be noted that for the entire study area, the temperature difference in one kilometer of thickness rarely drops below 20°C. This allows the use of the oceanic thermal energy throughout the region.

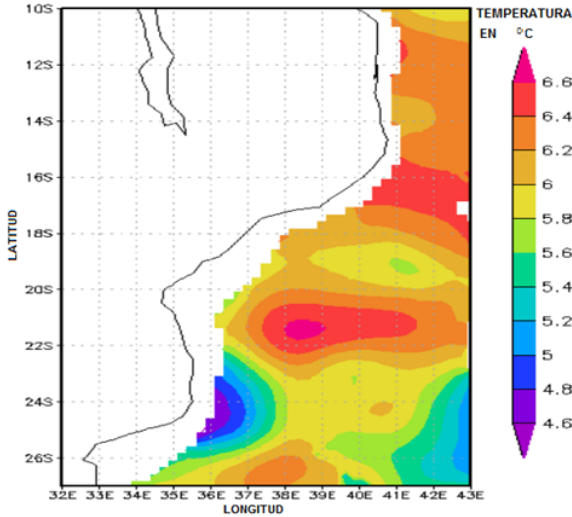


Figure 7. The annual temperature average in the deep waters of the MC.

Fig. 8 G, H, I shows the space distribution of the annual average of the SST for the year 2016, the temperature at the depth of 1000 meters and the isobaths from surface to 3000 m I. Note that the depths of 1000 m H, considered as an important characteristic to select the favorable regions for OTEC implantation in MC, are located very close to the coast in three zones of the north region, which are Angoche and Nacala (Province of Nampula), Pemba (Province of Cabo Delgado), and one of the southern region, Inhambane. The results for the northern region are analogous to those one obtained by [4], but in the present text another possibility for the southern region was identified.

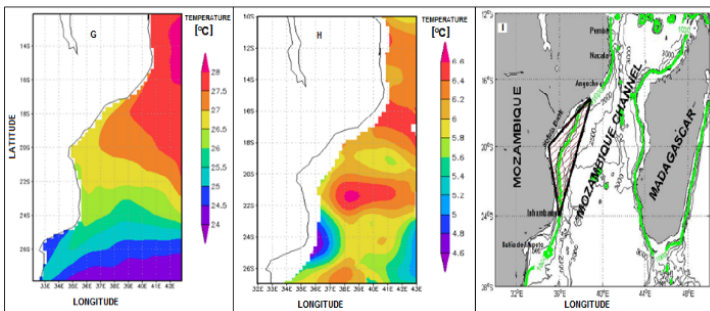


Figure 8. Presents the spatial distribution of the annual temperature average on the surface for the period 2016 (G), the temperature in the depth of 1 km (H), and the points with favorable premises for OTEC, where the green line presents the isobaths of 1000 meters (I).

The central region presents some limitations, such as: water cooling due to the presence of the water mass from the

Zambezi River, intense streams and a considerable distance of the isobaths of 1000 m. The Maputo Bay presents a similar situation; there converge five main rivers: Incomati, Umbeluze, Tembe and Matola to the West and the river Maputo to the South.

Table 2, presents the energy content averaged for the year 2016, the availability of this potential ocean energy is maintained almost during all the year and the Northern region is more active than the southern one.

Table 2. The content of energy in the water column, from surface to 1000 m depth.

Region	Locality	Energetic Content [J/m <sup>2</sup> ]
North	Pemba	88.922 * 10 <sup>6</sup>
	Nacala	87.756 * 10 <sup>6</sup>
	Angoche	87.756 * 10 <sup>6</sup>
South	Inhambane	84.460 * 10 <sup>6</sup>

### III.3. Severe events

Mozambique is exposed to the weather severe events due to its geographic location. Tropical cyclones and depressions, formed in the Indian Ocean, cross the Mozambique Channel and affect the coastal zone.

The hurricane season in Mozambique, is from November to April. Most of the tropical cyclones, that affect Mozambique, are formed in the Southern zone of the Indian Ocean near Madagascar from November to April. Tropical cyclones tend to emerge in the summer no matter where they occur. Fig. 9 shows the behavior of tropical cyclones from 1952 to 2007.

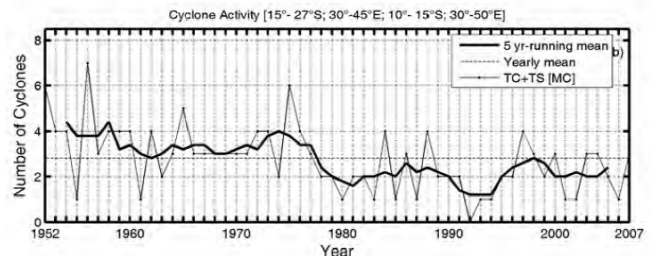


Figure 9. Number of tropical Cyclones (TC) and tropical storms (TS) in the MC, in the period 1952-2007 [17].

In this figure you can see the following:

- During the studied period, it can be observed as cyclones and tropical storms tend to decrease their effects in the MC, with a point of change at the end of the 1970s.
- The annual average of cyclone and tropical storm quantities that affected the MC from 1952 to 2007, is 2 or 3 cases in a year.

In Table 3, taken from [17], the frequencies of affectation are reflected by months.

It is observed that the most dangerous months are January and February, coinciding with the maximum sea surface temperature.

Table 3. Number of Cyclones and frequency in MC, (1980-2007).

Mozambique Channel (TC+TS)		
Month	Number	Frequency
November	2	0.07
December	7	0.25
January	18	0.64
February	16	0.57
March	8	0.29
April	5	0.18
Total	56	2.0

### III.4. Results of calculations

The calculation results of the pump power, the turbine power, the thermal efficiency of the Rankine cycle and the efficiency of the Carnot cycle are presented in Tables 4 and 5.

Table 4. Performance for Northern region (Pemba, Nacala, Angoche).

Region North Period (1981-2016)				
Surface T [°C]	Potency [MW]		Efficiency [%]	
	$\dot{W}_{pump}$	$\dot{W}_{turbins}$	$\eta_{thermal}$	$\eta_{carnot}$
Average-28.0	-0.5408	47.53	3.8	7.1
Maximum-28.8	-0.4772	48.96	3.9	7.7
Minimal-26.0	-0.5408	46.53	3.7	6.5
Period (2016)				
Average-28.0	-0.5408	47.53	3.8	7.2
Maximum-30.0	-0.0736	81.35	6.9	7.8
Minimal-26.0	-0.5408	46.53	3.7	6.6

The overall performance of these plants is low, not only because the thermal gradients are lower in general than are considered, but also because the technical limitations of several components of the installation (evaporators, condensers, pumps and turbines). These of efficiency are useful for evaluating the performance of a power plant compared to its maximum theoretical efficiency. The efficiency of the Carnot does not take into account the inevitable temperature losses in the heat exchanger.

Table 5. Performance for the southern region (Inhambane).

Region South Period (1981-2016)				
Surface T [°C]	Potency [MW]		Efficiency [%]	
	$\dot{W}_{pump}$	$\dot{W}_{turbins}$	$\eta_{thermal}$	$\eta_{carnot}$
Average-26.0	-0.5408	46.53	3.7	7.1
Maximum-27.9	-0.4772	48.96	3.9	7.7
Minimal-24.0	-0.3878	41.57	3.3	6.5
Period (2016)				
Average-26.5	-0.5408	46.53	3.7	7.2
Maximum-28.5	-0.5408	47.53	3.8	7.9
Minimal-24.0	-0.3878	41.57	3.3	6.5

The evaluation of the Carnot efficiency is not the best way to evaluate the different technologies of the thermodynamic energy generation, since it does not take into account the actual costs of the constructions and operations of the plant [14]. The efficiency of the Carnot's does not tell the whole story of any plant of power, because it is the absolute theoretical maximum, which is unattainable by plant of power any real world.

The results are promising for an OTEC plant. To pump water from a depth of 1000 meters, an incredible amount of work is required. However, the efficiency obtained is ideally enough to produce usable energy.

The power generation system through an OTEC plant can be compared to other plants such as wave, hydroelectric and diesel. Therefore, it is important to include capital, maintenance and service costs so that the technologies are equitable compared on an individual basis, as it is shown on Table 6, taken an example analyzed in Bali.

Table 6. Cost-per-unit comparison of OTEC with conventional energy sources [18].

	Plant Life [Years]	Capacity Factor [%]	Annual Output [GWh]	Cost Energy [US/kWh]
Wave	40	68	9	0.062-0.072
Hydro	40	48	5	0.113
Diesel	20	64	5	0.126
OTEC	30	80	8.8	0.149

## IV. CONCLUSIONS

Ocean thermal energy is available throughout the year in the northern and southern regions of the Mozambique Channel, while in the central region, near the mouth of the Zambezi River, and in Maputo Bay, where five major rivers converge, the surface is cooled too much by supply of the fresh water of the rivers, especially in the rainy season. The most suitable areas will be the population settlements of Pemba, Nacala, Angoche and Inhambane, not only because of the warmth of the adjacent waters trapped in the anticyclonic vortices, but also because of the proximity of the isobaths of 1000 m, depth where the temperatures are located from 4.6 to 6.8°C, which guarantee the difference of 20°C in contrast to the surface. This shortens the dimensions of the water conveyors and the electric cables, which lowers the installation costs. The possible impact of tropical cyclones, up to 4 on the Saffir - Simpson scale, should be taken into account, although the climate trend indicates a decrease in the frequency and intensity for the last 55 years. From the analysis of the yields, it can be seen that there is an average thermal efficiency of 6.9 to 3.3 % for the north and south regions respectively, and the Carnot efficiency of 7.1 to 7.9 %, which is considered as a good result, ideal for the power plant OTEC.

## V. RECOMMENDATIONS

For the next analogous studies, it is recommended to take into account the resistance of the OTEC material installation, the high salinity of the area (plus 35 psu) and the risk of occurrence of hurricanes, although these show a decrease in intensity and frequency. Because technologies are constantly being renewed, future studies should always analyze the costs of this technology, comparing them with the existing technologies and with the other options that are commonly used in the area of interest.

## REFERENCES

- [1] M. G. de C. Neves, "Estudo da Viabilidade de implantação de plantas para conversão da energia térmica do oceano (OTEC) no Brasil". MSc Thesis, Universidade Estadual Paulista, 2015.
- [2] I. Mitrani, *Meteorología Marina*, digital book, 1st Ed., (Instituto de Meteorología, Agencia de Medio Ambiente, CITMATEL, 2017), pp. 88-90.
- [3] A. Achkienasi, and I. Mitrani, *Rev. Cienc. Tierra y Esp.* **17**, 130, (2016).
- [4] L. Hammar, J. Ehnberg, A. Mavume, B. C. Cuamba and S. Molander, *J. Renew. Sustain. Energy* **16**, 4938, (2012).
- [5] S. Goto, Motoshima, T. Sugi, T. Yasunaga, Y. Ikegami, and M. Nakamura, *Electr. Eng. Jpn.* **176**, 272, (2011).
- [6] R. Satre, and A. Da Silva, *Rev. de Inv. Pesq.* **3**, 3, (1982).
- [7] M. W. Schouten, W. P. M. de Ruijter, P. J. van Leeuwen and H. Ridderinkhof, *Deep-Sea Res. Part II-Top. Stud. Oceanogr.* **50**, (2003).
- [8] I. Mitrani, A. Moreno, and O. Padilla, *Tropicheskaya Meteorologuia*, (Guidrometeoizdat, Leningrado, USSR, 1985), pp. 186-191.
- [9] F. J. Millero, G. Perron, and J. F. Desnoyers, *J. of Geophys. Res.* **78**, 4499, (1973).
- [10] N.P. Fofonoff and R.C. Millard, *Algorithms for Computation of Fundamental Properties of Sea Water*. UNESCO Technical Papers in Marine Science, **44**, 44, (1983).
- [11] R. H. Stewart, *Introduction to Oceanography*, (Texas A. and M. University, Texas, 2008), pp. 50-52.
- [12] M. J. Moran and H. N. Shapiro, *Fundamentals of Engineering Thermodynamics*, 5th Ed. (The Ohio State University, Ohio, USA, 2006). pp. 321-328
- [13] W. Engels and F. Zabihian, *ASEE Zone I Conference, Principle and Preliminary Calculation of Ocean Thermal Energy Conversion*, (University of Bridgeport, Bridgeport, USA, 2014).
- [14] C.R. Upshaw, "Thermodynamic and Economic Feasibility Analysis of a 20 MW Ocean Thermal Energy Conversion (OTEC) Power Plant". MSc Thesis, University of Texas, 2012.
- [15] J. R. E. Lutjeharms, *The Coastal Oceans of South-Eastern Africa*, In *The Sea*, (Harvard University Press, Cambridge, USA, 2006), pp. 783-834.
- [16] C. Sete, J. Ruby, and V. Dove, *Seasonal Variation of Tides, Currents, Salinity and Temperature along the Coast of Mozambique*, UNESCO (ICO), (Centro Nacional de Datos Oceanográficos, Mozambique, 2002).
- [17] A. F. Mavume, L. Rydberg, M. Rouault and J. R. E. Lutjeharms, *Western Indian Ocean*, *J. Mar. Sci.* **8**, 15, (2009).
- [18] A. R. Sinuhaji, *Potential Ocean Thermal Energy Conversion (OTEC) in Bali* [ISSN 2413-5453], **1**, (2015).

---

This work is licensed under the Creative Commons Attribution-NonCommercial 4.0 International (CC BY-NC 4.0, <http://creativecommons.org/licenses/by-nc/4.0>) license.

